Applied Physics A –Materials Science & Processing, Online First™ , 2008
The original publication is available at www.springerlink.com

Optical Coherence Tomography in Art Diagnostics and Restoration

Piotr Targowski[1], Bogumiła Rouba[2], Michalina Góra[1],
Ludmiła Tymińska-Widmer[2], Jan Marczak[3], and Andrzej Kowalczyk[1]

[1]Institute of Physics, Nicolaus Copernicus University, ul. Grudziądzka 5, 87-100 Toruń, Poland

[2]Institute for the Study, Restoration and Conservation of Cultural Heritage, Nicolaus Copernicus University, ul. Gagarina 9, 87-100 Toruń, Poland

[3]Institute of Optoelectronics, Military University of Technology, ul. Kaliskiego 2, 00-908 Warszawa, Poland

Corresponding author: P. Targowski, ptarg@fizyka.umk.pl, fax: +48 56 622 5397, phone: +48 56 611 3206

Received: 25 June 2007/Accepted: 15 January 2008

Abstract

An overview of the technique of optical coherence tomography (OCT) is presented, and a Spectral OCT instrument especially designed for art diagnostics is described. The applicability of OCT to the stratigraphy of oil paintings is discussed with emphasis on examination of the artist's signature. For the first time, OCT tomograms of stained glass are presented and discussed. The utilisation of Spectral OCT in real-time monitoring varnish ablation is discussed with examples of ablation, melting and evaporation, and exfoliation of the varnish layer provided, for the first time.

PACS Numbers: 42.30.-Wb, 07.60.-j, 07.60.-Ly, 81.70.Fy, 79.20.Ds

1. Introduction

Scientific examination of artworks often plays an important role in technical or historical research, and can also assist in conservation and restoration treatments. A detailed knowledge of the physical structure of the artwork provides a basis for evaluation of its authenticity and attribution, as well as recognition of the origins of any decay and of conservation and/or restoration requirements. Determination of the stratigraphy of these complex objects is one of the most important procedures. Cross-sectional images of the structure under examination provide an enormous amount of data on composition, sequence, thickness and state of preservation of different elements of the artwork, and serve as a reference point for the results of other chemical and physical examinations.

The classic approach to obtain information about a layered structure of an art object starts from observations of its surface. Natural cross-sections visible at the edges of voids as well as broken pieces are often used in such investigations. Unfortunately, access to structural information obtained in this way is not usually sufficient, due to the limited, chance choice of their location as well as to weathering of the surface. Microscopic observation techniques (including stereomicroscopy [1], polarized light microscopy [2-5], and fluorescence microscopy [6]), together with various microanalytical techniques [7-9] applied to cross-sections of micro-samples taken from the object [10], therefore provide the most comprehensive information on its stratigraphy. However, sample acquisition is plainly invasive, resulting in destruction of the integrity of the artwork. For that reason it must be strictly limited as to the location, size and number of samples collected.

Increasing attention is therefore being given to alternative non-invasive and non-contact methods of analysis originating from spectroscopy, reflectography, fluorescence or radiography. However the majority of such techniques deliver rather selective information. Data on structural complexity obtained with one method is either not detailed enough, considers only selected layers or structural elements visible at the surface of the object, or is integrated over the whole thickness of the artwork. Only a few techniques have been applied up to now to estimate the sequence and thickness of layers in artwork structures, and these are not without their limitations, e.g., in the case of high-energy proton-induced X-ray emission (PIXE), the problems are associated with distinguishing layer sequences containing more complex mixtures of pigments [11]. Confocal laser scanning microscopy (CLSM), permitting optical sectioning, however, is one of the rare exceptions enabling production of a three-dimensional images of the internal structure of delicate oil paintings and textile fibres, in this case even down to submicron resolution. CLSM can be carried out with both visible and ultraviolet light [12-14]. However, the depth of imaging is limited by the range over which light can propagate in the media examined, and the investigated field is very small which makes testing of a large area very time consuming.

Optical sectioning can also be performed by means of Optical Coherence Tomography (OCT). This is a relatively new, but nevertheless well–established, technique that offers a unique possibility for determination and visualization of the inner structure of semi-transparent objects which weakly absorb and scatter light. It is non-contact, non-invasive and, most importantly, safe for the objects tested as long as the exposure is limited to a certain level. Over the last four years, an increasing number of applications of various modalities of the OCT technique to investigate the structure of cultural heritage artifacts have been reported and reviewed recently [15]. One of the first applications of OCT was the imaging and indication of structural differences in glaze layers on porcelain and faience objects [16,17] as well as in original and fake archaic jade artifacts from the Qijia and Liangzhu cultures in China [18]. Nevertheless, most applications considered have been for the examination of easel-painting structures. Independent experiments have established the applicability and efficacy of OCT in obtaining, in a non-destructive way, well-enough resolved cross-sectional images of varnish layers to enable precise measurements of their thicknesses [15,17,19-22] and to accurately monitor changes in the varnish surface profile during the drying process [23]. Systematic studies on the applicability of OCT using different light sources to stratigraphic examinations of different paint layers have also been made [23-25], together with tests of its ability to image underdrawings covered by the paint layers [22].

The high speed of data collection which distinguishes the spectral domain variant (see below) of OCT (SOCT) has made possible application of the method to recovery of surface profiles and varnish thickness maps from a series of parallel cross-sectional images [26,27]. Preliminary tests demonstrated that, due to the high speed of data acquisition, SOCT may also be applied to real-time simultaneous monitoring of in- and out-of-plane deformations of easel-painting surfaces in response to environmental fluctuations [17,28,29] and that, moreover, it can be useful for establishing conditions for laser ablation of the varnish layer [30,31].

In the present contribution, the physical foundations of the OCT technique will be presented and instrumental details described. The application of OCT to stratigraphic examination of oil paintings will then be discussed, with particular reference to imaging of glaze and varnish layers and to the examination of author signature areas. Apart from its application to paintings, the OCT method may also be useful in the imaging of stained glass. This application, as well as utilisation of the fast, spectral version of the OCT technique to the recording of laser ablation of samples of varnish from paintings, will be described for the first time.

2. The method

OCT relies on the examination of light reflected back from the internal structures of the object monitored. The information obtained as to the back-scattering intensity and its time delay enables reconstruction of a single optical scan (the A-scan) representing the locations of back-scattering and reflecting points distributed within the object along the path of the penetrating beam. Serial lateral

displacement of the beam to adjacent positions enables imaging of the structure of a two-dimensional slice of the object (B-scan).

The time delay is measured indirectly by means of the interferometry. The common intensity $I(\omega)$ of two superimposed beams of monochromatic light reflected or scattered back from the sample (intensity I_s) and reference mirror (intensity I_r) is given by:

$$I(\omega) = I_s(\omega) + I_r(\omega) + 2\sqrt{I_s(\omega) I_r(\omega)}\cos(\omega\tau_{rs}) = S(\omega)\left[R_s + R_r + 2\sqrt{R_s R_r}\cos(\omega\tau_{rs})\right] \quad (1)$$

where $\tau_{rs}=2\Delta z_{rs}/v$ is the time delay between sample and reference beams caused by the difference in distances from the beam splitter (see Section 3. Instrumental details, below), $S(\omega)$ is the spectrum of the light source, R_s and R_r are reflection coefficients from the sample and reference mirror, respectively. OCT uses broad band light sources (of low time, but high spatial coherence) and two detection schemes: the standard Time Domain and the, more recent, Fourier Domain, to derive the locations of the reflecting or back-scattering object.

First generation OCT systems use Time domain detection, and are therefore also known as Time domain OCT (TdOCT) systems. The signal is integrated over all optical frequencies on the photodiode:

$$\begin{aligned} I &= \int I(\omega)d\omega = (R_s + R_r)\int S(\omega)d\omega + 2\sqrt{R_s R_r}\,\mathrm{Re}\left[\int S(\omega)\exp(i\omega\tau_{rs})d\omega\right] \\ &= (R_s + R_r)\int S(\omega)d\omega + 2\sqrt{R_s R_r}\,\mathrm{Re}[\Gamma(\tau_{rs})] \end{aligned} \quad (2)$$

ReΓ(τ) is an oscillatory function with an envelope obtained from the Wiener-Khintchine relation between the light spectrum S(ω) and its coherence function Γ(τ) [32]. The axial resolution of OCT is determined by the width of the envelope of ReΓ(τ): $\frac{2\ln 2}{\pi}\frac{\lambda_{centre}^2}{\Delta\lambda}$ (where Δλ is the full-width-half-maximum bandwidth and λ_{centre} is the centre wavelength), divided by the group refraction index of the media imagined. Use of light with a broad spectrum of near-infrared optical wavelengths (700 – 1100 nm) enables imaging with high resolution: up to 2 μm, in media of refractive index 1.5.

The function ReΓ(τ) reaches a maximum when the distances to the beamsplitter from the sample point monitored and the mirror are equal (τ_{rs} = 0). Therefore, during a scan, involving a controllable variation in the optical length of the reference arm, short oscillatory pulses are detected, centred at times when the position of the reference mirror corresponds to the position of the back-reflecting interface or back-scattering point inside the object. In this way, a single A-scan representing one line of the tomogram is achieved.

Almost a hundred-fold increase in the imaging speed over TdOCT systems has been attained by recently developed novel OCT technology. This new technique employs Fourier domain detection, and is therefore referred to as Fourier domain OCT (FdOCT). Here, the entire information about the single axial line (A-scan) of the object measured is extracted from the spectral fringe signal: instead of collecting the integrated signal on a single detector, the broadband light is analyzed by a spectrometer equipped with an array of photodetectors (line CCD), and the array of intensities recorded numerically processed by a PC using Fourier transform (FT) methodology:

$$FT\left[I(\omega)\right] = \left(R_s + R_r\right)FT\left[S(\omega)\right] + 2\sqrt{R_s R_r}\,FT\left[S(\omega)\cos(\omega\tau_{rs})\right] = \left(R_s + R_r\right)\Gamma(\tau) + 2\sqrt{R_s R_r}\,\Gamma(\tau \pm \tau_{rs}) \tag{3}$$

The resulting signal, obtained from a single exposure, provides directly the magnitude and time-delay of light back-scattered or back-reflected from the internal substructure of the object measured with respect to stationary reference mirror. The main features of this method are that it does not require moving parts for axial scanning and that it collects light from all layers at once. This results in improved stability and, due to the multiplex advantage [33], more efficient use of the light collected. In effect, despite almost a 100-fold reduction of the examination time, there is a considerable increase in detection sensitivity.

It is possible to achieve higher scan speeds in TdOCT systems, up to several thousand axial scans per second, by using advanced methods of mechanical scanning. In TdOCT, however, increased imaging speed and/or improved axial image resolution cause an automatic decrease in detection sensitivity. Standard FdOCT (being equipped with a spectrometer, it is also therefore more commonly referred to as Spectral OCT, or SOCT) provides speeds of 20 thousands of A-scans per second without this loss in sensitivity. Moreover, very recently developed FdOCT systems based on a swept light source allow the achievement of as high as 370 thousands scans per second.

High speed may be exploited in several ways. Firstly, it is possible to increase the A-scan density in the individual tomogram. Because of speckle averaging, the tomogram demonstrates dramatic improvement in quality as well as greater freedom from sample motion artifacts. Secondly, one may collect many cross-sections of lower A-scan density, but at different locations, to build up a 3-D image of the structure within a reasonable time. Again, if cross-sections are taken in the same place, cross-sectional movies of deformations of various details of a structure are obtained. With this unique possibility, close insight into the dynamics of structural details under the influence of environmental changes such as temperature and humidity can be gained.

3. Instrumental details

The OCT data presented in this manuscript were obtained with a prototype Spectral OCT instrument constructed at the Nicolaus Copernicus University. An optical schematic of the Spectral OCT system is shown in Figure 1. For standard measurements at a resolution of 10 μm (in a medium of refractive index 1.5), a broadband ($\Delta\lambda$ = 50 nm, central wavelength 830 nm) superluminescent diode (LS) was employed as the light source. A higher axial resolution of 2 μm in the object (see Figure 5b in the results section) was achieved by using a combination of three SLDs, which together emit light of a wavelength span up to 190 nm centred at 870 nm.

The light is launched in a parallel beam into the Michelson interferometer, where it is split into reference and object arms. To minimise dispersion broadening, the open air configuration of the interferometer was chosen. The light in the reference arm is attenuated by a neutral density filter (NDF) and passed, if necessary, through the pair of prisms acting as an adjustable dispersion corrector (DC). Finally, it is reflected back from the stationary reference mirror (RM). The sample arm is terminated by the optical scanning head, which enables the probe beam to be scanned across the object in two lateral directions by an electronically controlled pair of galvanometric scanners (X-Y). A lens focuses the light onto the sample, and the pivot of the galvanometric scanner placed in the focal plane of the lens enables parallel transverse scanning of the sample. The light beams returning from the reference mirror and from the sample are brought to interference at the output of the interferometer and analyzed by a customized spectrometer. This comprises a high speed line-scan camera (CCD) and a highly efficient reflective holographic grating (DG) with 1800 grooves/mm. The entire interferometer, together with the scanning system and the spectrometer, is mounted on an adjustable stand. The acquisition process and scanning protocols are controlled by a custom-designed compact electronic driving unit.

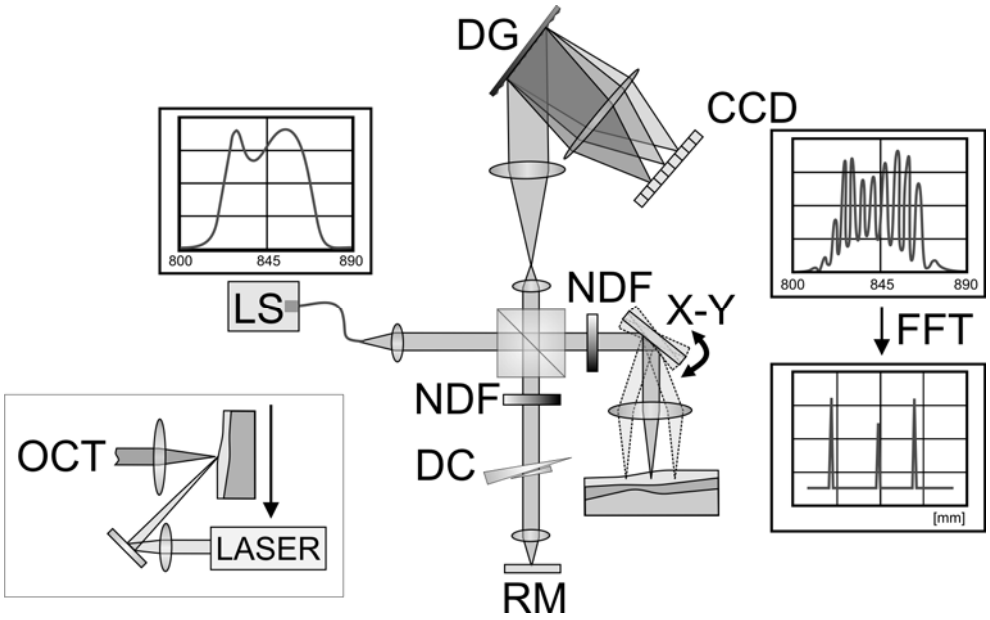

Fig. 1. Diagram of the instrumental set-up: LS – light source, RM – reference mirror, DG – diffraction grating, NDF – neutral density filter, DC – dispersion compensator, CCD – CCD line-scan camera, X-Y – galvanometric scanner. Insert: a combination of the OCT instrument with an ablation laser.

The sensitivity of the system is 80 dB. The axial resolution of the instrument is either 2 μm or 10 μm – for high and low resolution variants, respectively – while the transverse resolution is kept better than 15 μm. The axial range of imaging is 2 mm, and it depends both on the number of pixels in the camera and the depth of focus of the optics utilised in the scanning head. The in-plane field of view is about 15 mm square: despite the aperture of the focusing optics, a significant decrease in back-scattered signal is observed beyond these perimeters. The optical power of the beam incident at the surface of the object is between 200 and 750 μW. The exposure time is 32 μs per single A-scan.

Together with a scanning beam to document the precise location of the point of examination, an additional industrial camera coupled to the OCT instrument registers the surface of the object.

A number of scanning protocols for use in structural analysis have been elaborated. In order to reveal more detailed structure, a high density single cross-section of 5 mm length composed of 5000 A-scans is acquired. The total measurement time for such a two-dimensional cross-sectional image (B-scan) is thus 0.16 seconds. To obtain a general insight into the 3-D structure of the object, 200 cross-sectional images, each consisting of 2900 A-scans, covering an area of 5 × 5 mm, are acquired. The total measurement time for this protocol is less than 20 seconds. A variant of this protocol used for studies of signatures covers an area of 14 mm × 16 mm with the same number of A-scans. The data are stored in raw digital form and analyzed after each measurement session.

In addition to this high resolution imaging, the OCT system utilised in this study permits *real-time* low density imaging. In this mode, a cross-section comprising 200 A-scans is displayed and refreshed 5 times per second. The size, and thus also the quality, of the image is predominantly limited here by computing speed.

Preliminary tests of OCT-tracking of varnish layer removal by laser ablation were carried out using an Er:YAG (erbium-doped yttrium-aluminium-garnet, Er:$Y_3Al_5O_{12}$) laser [34,35] emitting infrared radiation at λ = 2936 nm. This was combined with the SOCT system (Fig. 1, insert) to enable on-line monitoring and *in-situ* control during each stage of the laser ablation. In this procedure, OCT movies composed of 300 cross-sections (frames) of 8 mm length, each comprising 2000 A-scans, were collected during the 20-second experiment at a rate of 15 frames/sec. These movies document the ablation process, showing in real time the creation of the ablation crater or – during the next stage of the experiment – continuous removal of the varnish layer. The latter was accomplished by

continuously translating the sample in the plane of the painting surface whilst concurrently applying the laser pulses. For the translation rate of 0.4 mm/s used, the 2 Hz pulse frequency and the ~2 mm diameter beam spot of the ablation laser meant that each point on the sample was irradiated 10 times.

In all OCT tomograms shown in this study, the intensity of light scattered and/or reflected from the internal structures within the sample is coded in a gray scale. Darker shades of gray indicate a higher level of scattering or reflection of the probing light, while lighter ones indicate lower scattering levels. In all of the tomograms presented, light is incident from above, and the interface between air and the sample is thus always the uppermost line.

To improve visual interpretation of the tomograms, the in-depth (vertical) scale is expanded. In all tomograms presented, it is also corrected for the group refractive index of the medium imaged, assumed here to be equal to 1.5. This correction is occasioned by the fact that all originally measured distances are optical ones, converted thereby to their true length equivalents.

3. Results

3.1. Structural analysis of paintings

Resolution of the multi-layer structure of oil paintings is important in understanding their history and present condition. It is also a necessity if any conservation treatment is planned. An efficient, easy-to-use and preferably non-invasive method of examination is therefore much to be desired. Optical Coherence Tomography is fast and non-contact, and thus may be applied as many times as necessary at various locations in the picture. The major restriction arises from the limited permeability of the structure investigated to infrared light. However, in many cases the multi-layer internal structure of the painting is detectable. If it is covered by a varnish layer thick enough to be resolved with a particular OCT system, the varnish is visible as a dark, non-scattering strip just under the surface of the painting. The recognition of this layer is thus usually unequivocal. The identification of the successive strata – of semi-transparent paint layers – can be more challenging. For interpretation of such an image, the use a reference key for proper assignment of structures visible in tomogram to the components of the painting is recommended. Such a reference can be realised by other methods of investigation, such as UV-fluorescence observation revealing the presence of varnishes and some glazes, as well as microscopic examination in locations of structural damage (losses or abrasions of upper layers) providing information on the stratigraphy of the painting. If an OCT examination is performed before taking samples for chemical investigation, the cross-sectional microphotography of a single sample – taken at location where it is possible to image the structure of the painting by OCT – can serve as the best reference key for tomogram interpretation. Once all of the strata have been identified, OCT tomograms taken at various places provide information on the structure of the painting over a larger area .

The results of such a procedure are illustrated in Figure 2, in which a series of OCT tomograms registered in parallel over an area of 7 × 7 mm is shown. After the OCT examination, a classical sample was collected from this site and analysed microscopically: both visible reflected light and UV induced fluorescence were registered. Direct comparison between the image of the sample and the respective fragment of the OCT tomogram (dashed frame) permits identification of the strata imaged, namely varnish and single glaze layer. However, closer analysis of all of the tomograms, especially of those in the regions marked out with dots, leads to the conclusion that the structure and thickness of the varnish and glaze layers in the object investigated change very rapidly, and that a single classical sample (of size less than one square millimetre) may not be representative of a larger area of the painting even in its vicinity. Structural information provided in this way may thus suffer from significant uncertainty. This failing may be overcome by carrying out in parallel an OCT examination which, being non-invasive, may be repeated as many times as desired, and provides cross-sectional images from a much larger area in any chosen section of the picture.

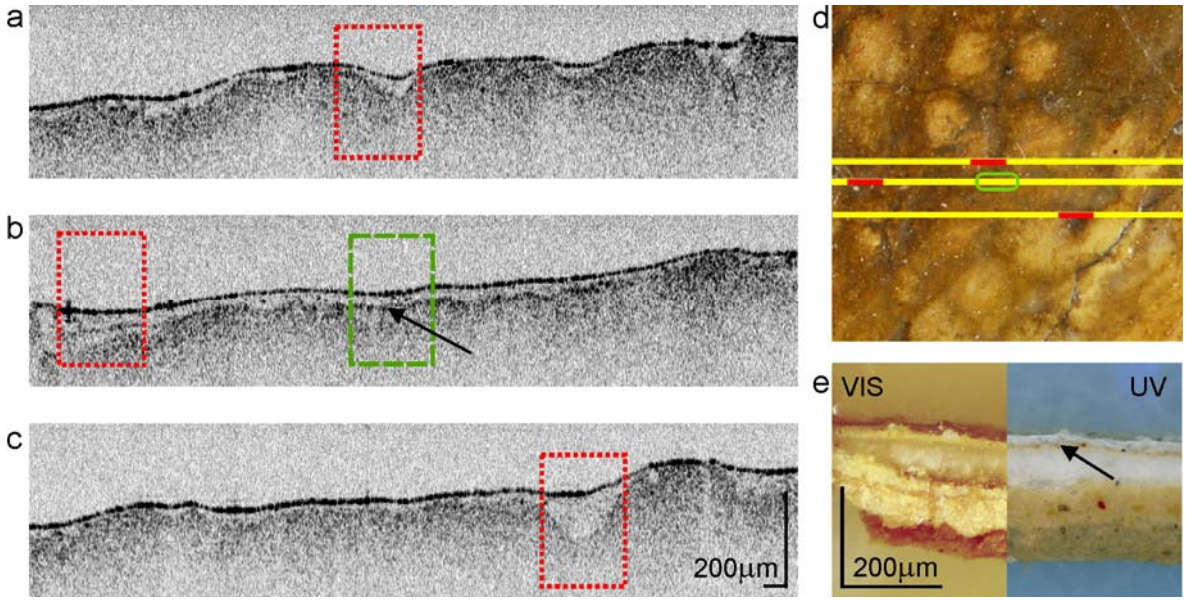

Fig.2. Stratigraphic OCT images (a,b,c) taken at three nearby locations in the same sample (d). The dashed frame in Fig. 2b indicates the area shown also as a microphotograph (e) of the cross-section of the sample taken in this location after OCT examination. Dotted frames indicates areas of evidently different structure.

The efficacy of OCT in structural imaging is limited by the transparency of the pigmented strata. Fortunately, even old and yellowed varnishes are transparent enough to be penetrated by the infrared light used for OCT imaging. Such examination, especially if performed over a large area of the painting, can provide comprehensive information about the varnish layer thickness, which can then be compiled into thickness maps or histograms [27].

Non-invasive imaging of the varnish layer with the aid of OCT finds a promising application in investigation of the area of the author's signature, which is considered inviolable and, in order to preserve it in as intact and pristine state as possible, under no circumstances to be examined other than non-invasively.

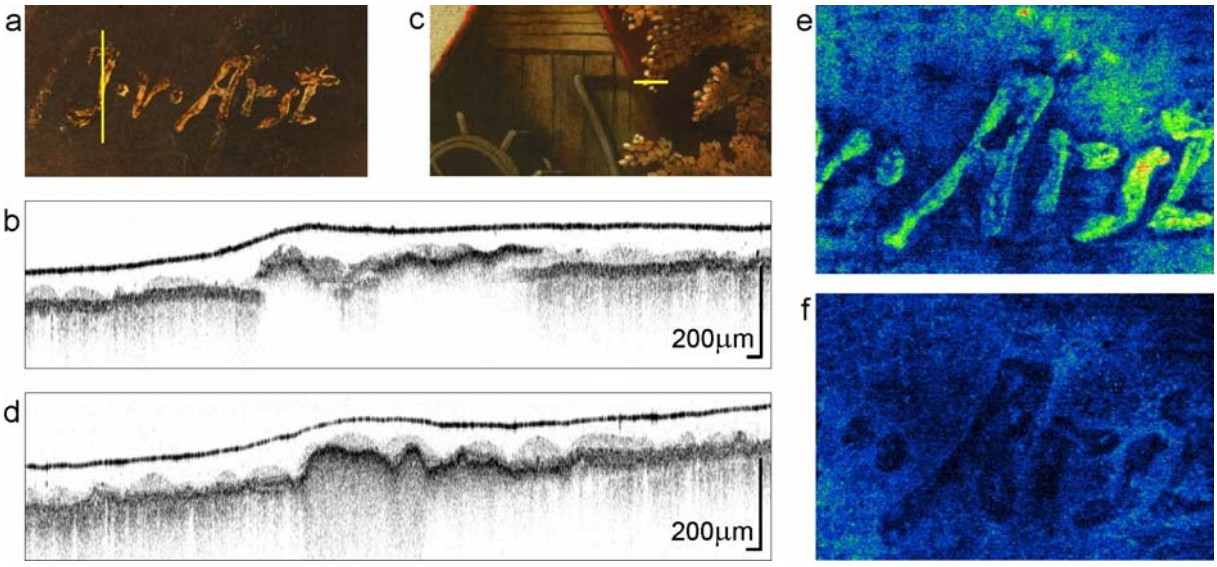

Fig. 3. The signature investigated (a); the bar indicates the place at which a SOCT tomogram (b) was recorded. Another part of the same picture (c) for comparison, with the location of the respective tomogram (d) again indicated by the bar. Image of the signature obtained by integration of the OCT data collected from depths between 60 µm and 128 µm under the surface (e). The shadow cast by the signature over the paint recovered from the signal arriving from depths greater than 128 µm (f).

In particular, to avoid future controversy, the abstraction of samples of it, must be strongly limited. The analysis of this region is important both in correctly attributing the work and in confirming its authenticity.

The most routine current examination of the integrity of paintings is based on the well-known ability of old varnishes and binding media to exhibit visible fluorescence when illuminated with UV radiation. Loss of integrity of the area due to late interventions are visible in this method as darker, non- or less-fluorescing stains. A common method of counterfeiting signatures is thus to paint it on the original varnish layer and then cover it with ageing lacquer exhibiting strong UV-induced fluorescence. A non-invasive method permitting differentiation of layers of various optical properties could therefore be very useful in detecting such counterfeiting.

In Figure 3, a test designed to exhibit the ability of OCT to resolve the location of a signature within the layer sequence is presented. It was carried out on a 20th-century copy of a landscape performed in the manner of 17th-century Dutch masters. The signature (Fig. 3a) has been painted onto the original varnish and then covered intentionally with covering layer of UV fluorescing lacquer. The routine UV examination did not indicate that it was fake: the whole surface of the painting fluoresced evenly. However, OCT examination (Fig. 3b) revealed clearly that the signature is located in a separate stratum, above the paint layer. The most characteristic features are the edges of the paint strokes forming the signature, which cause it to seem to float above the lower, original layer. This is not the case for original impastos (Fig. 3c), a tomogram of an example of which is shown in Figure 3d for reference. For unambiguous identification, 3D data collected in the area of the signature may be analysed in an alternative way: the signal recorded from defined depths beneath the surface of the painting may be added together and displayed as a false-colour intensity image. From this it is seen that the signature itself is contained in the signal collected from depths between 60 μm and 128 μm (Fig. 3e), whilst the signal collected from below this reveals the paint surface together with a shadow on it cast by the signature (Fig. 3f).

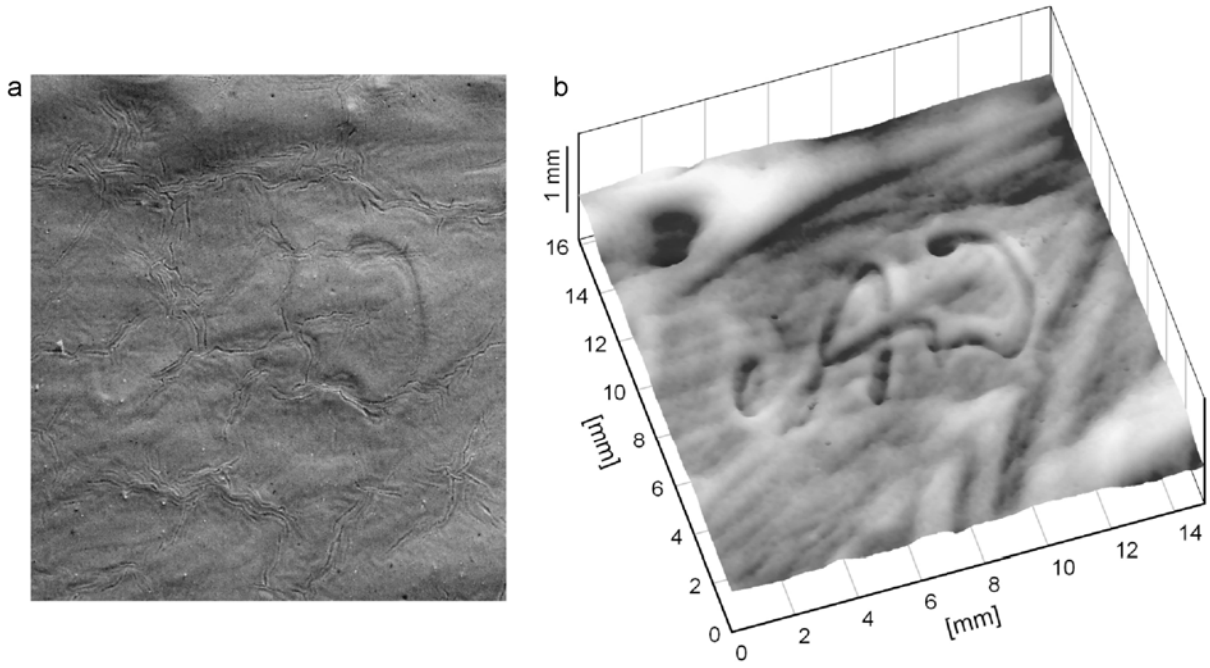

Fig. 4. Oblique-light photography of the signature incised in fresh paint and then covered by a thick varnish layer (a). A false-colour altitude map of the paint surface recovered by OCT (b).

The ability of OCT to collect volume data may also be utilised to reveal convex or concave details in the paint layer when the surface texture has been levelled by a thick varnish, especially when these are not clearly recognizable by other methods, e.g., observation in oblique light. In Figure 4, a test

painting is shown, on which a concave signature was incised with a wooden stick in an fresh acrylic impasto. After drying, the paint layer was covered with two layers of Ageing Varnish (Lefranc&Bourgeois) and a single layer of matt varnish (acrylic 115, Talens). This rendered the carved signature hardly legible, even under oblique illumination (Fig. 4a). To reveal the details of the signature, an area of 14 × 16 mm containing it was scanned by OCT at a resolution of 200 × 2900 points. Profiles of the surface of the picture and the paint-varnish interface (Fig. 4b) were recovered, the latter being shown as a false-colour altitude map with lighter shades of grey indicating more elevated areas. The improvement in legibility of the signature is evident.

3.2. Structural analysis of stained glass

Historical glass exemplifies media from which collecting samples is virtually impossible. In the case of glass windows, stratigraphic examination has been limited to the edges of sheets taken out of frames. Unfortunately, these parts are usually protected from environmental impact and therefore again are not representative of deterioration in the object as a whole.

Similarly, if colours were painted onto the glass and then annealed in a furnace, this composite structure has up to now been difficult to analyse non-destructively. It seems that here too, OCT offers an interesting alternative. In Figure 5a, a central portion of a 19th-century glass window painted with annealed colours is depicted. The high resolution tomogram (Fig. 5b) has been collected across three areas – from left to right: a semi-transparent, thick green annealed paint with a highly scattering surface, a strongly absorbing black area, and a non-absorbing glass covered by a thin yellow glaze. As one can see from the tomogram, the cross-section of the green layer is well revealed, whilst only the surface of the black one can be differentiated. However, glass offers the unique opportunity of imaging the same area not only with light approaching from the paint layer side (solid arrows in Fig. 5c), but also with light penetrating through the whole, here 3.5 mm thick, supporting glass (dashed arrows in Fig. 5c). The tomogram obtained in this way is shown in Fig. 5b, lower panel. Now the opposite surface of the non-transparent black layer can be seen. The two images may thus be combined together (Fig. 5c) and the thickness of the non-transparent black layer recovered.

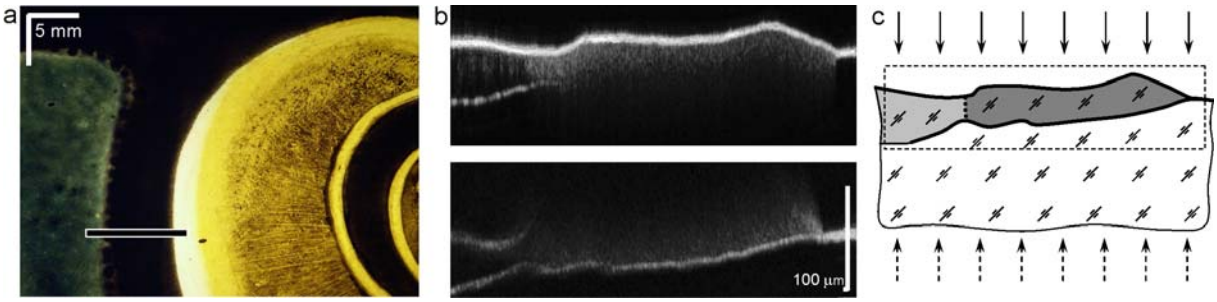

Fig. 5. An example of OCT examination of a stained glass window (a). The bar indicates the location of the SOCT examination (b). The upper tomogram was obtained with illumination of the painted side (solid arrows in graph c). The lower tomogram was recorded through the supporting, 3.5 mm-thick, glass (dashed arrows in graph c). By combining both images (b), the shape of the non-transparent black layer may be recovered (c).

It is worthwhile noting that obtaining of a sharp tomogram with illumination through the supporting glass (Fig. 5d) requires correction for the dispersion of the glass. This is accomplished by introducing an additional block of BK7 glass of adjustable thickness (Fig. 1) into the reference arm of the interferometer.

3.3. Functional imaging

Fourier domain OCT methods are very fast. Currently available linear cameras are able to collect and transfer to the controlling computer as many as 30,000 spectra per second (instruments equipped with sweep-source lasers are even able to increase this by up to ten-fold). Hence spectral (linear camera-based) systems are potentially capable of handling as many as 10-15 high density cross-sectional images (B-scans) per second. Unfortunately, even the most modern personal computers, with 4 GHz processors, are still not able to process such an amount of data fast enough for real–time monitoring. However, rapid progress in digital technology, together with more efficient software, should overcome this limitation before long. Therefore it is reasonable to assume that real-time high-density imaging with OCT will be available for a moderate price in the not-too-distant future.

The instrument described in this paper collects, and stores for further post-processing, high density B-scans at a rate of 15 images per second. An example of a process whose dynamics could be studied at such a frame rate is laser ablation of varnish from oil paintings. The application of lasers for varnish removal has been being tested over the last ten years or so [36], and this method, is slowly becoming an alternative to the traditional mechanical and chemical techniques in certain cases. Since the varnish layer is usually inhomogeneous in thickness and structure, an effective method of on-line monitoring of ablation is needed in order to accomplish complete ablation of the varnish while preventing ablation of the underlying paint layers. When operating UV lasers which efficiently generate a plasma during the ablation, Laser Induced Breakdown Spectroscopy (LIBS) is usually used as a tracking tool [37,38]. This method, however, has two disadvantages. Firstly, ablation is terminated when traces of pigments from the paint layer are detected, and consequently this method can not be used if only partial removal of the varnish layer is desirable. Secondly, when operating with IR lasers, plasma is usually not generated, so that LIBS cannot then be employed to monitor the ablation.

The OCT method, based on direct imaging of the varnish layer, is in principle free of these disadvantages. Some preliminary tests using OCT as a tracking device have therefore been carried out. For this study, three specially prepared samples were chosen to demonstrate the ability of OCT to reveal different processes which may occur during the ablation treatment. In all of the samples, a cardboard support was covered with a paint layer and, after drying, a varnish layer was applied. One of the samples was prepared with an acrylic paint and Dammar Matt Varnish (Maimeri), and tested soon after drying. The two remaining samples were prepared one year before examination and subjected additionally to environmental weathering for four weeks in a climate chamber (KPK 630.V, VEB Feutron Greiz, Niemcy, T range from 10 to 30 °C, RH range from 20 to 80 %). These were of oil paint together with varnishes by Talens: one with Acrylic Varnish Mat 115, the other with Picture Varnish Glossy 002 (ketone). All the samples were also sprayed with a thin layer of matt Winsor & Newton varnish in order to reduce mirror reflections during testing.

A detailed account of these experiments and procedures may be found elsewhere [31,39]. Briefly: ablation conditions, namely fluence and spot size, were adjusted for each varnish–laser combination to values that enabled partial removal of the varnish only, and permitted preservation of a thin layer of the coating on the surface of the paint layer. The laser pulses were then applied to the sample while it was being translated in the plane of its surface. The whole process was monitored by SOCT tomography and 20-second tomographic movies of the process recorded.

In Figure 6a, one frame from such a movie, typical for ablation of the artificially weathered ketone varnish, is presented. During the process, the sample is translated to the left, laser pulses impinging always at the centre of the image. The original, not yet ablated, varnish layer is visible to the right, whilst the partially ablated layer extends to the left. In this case, removal of the varnish layer occurs very precisely. The layer is thinned down to the desired thickness without any undesirable effect on the underlying paint layer.

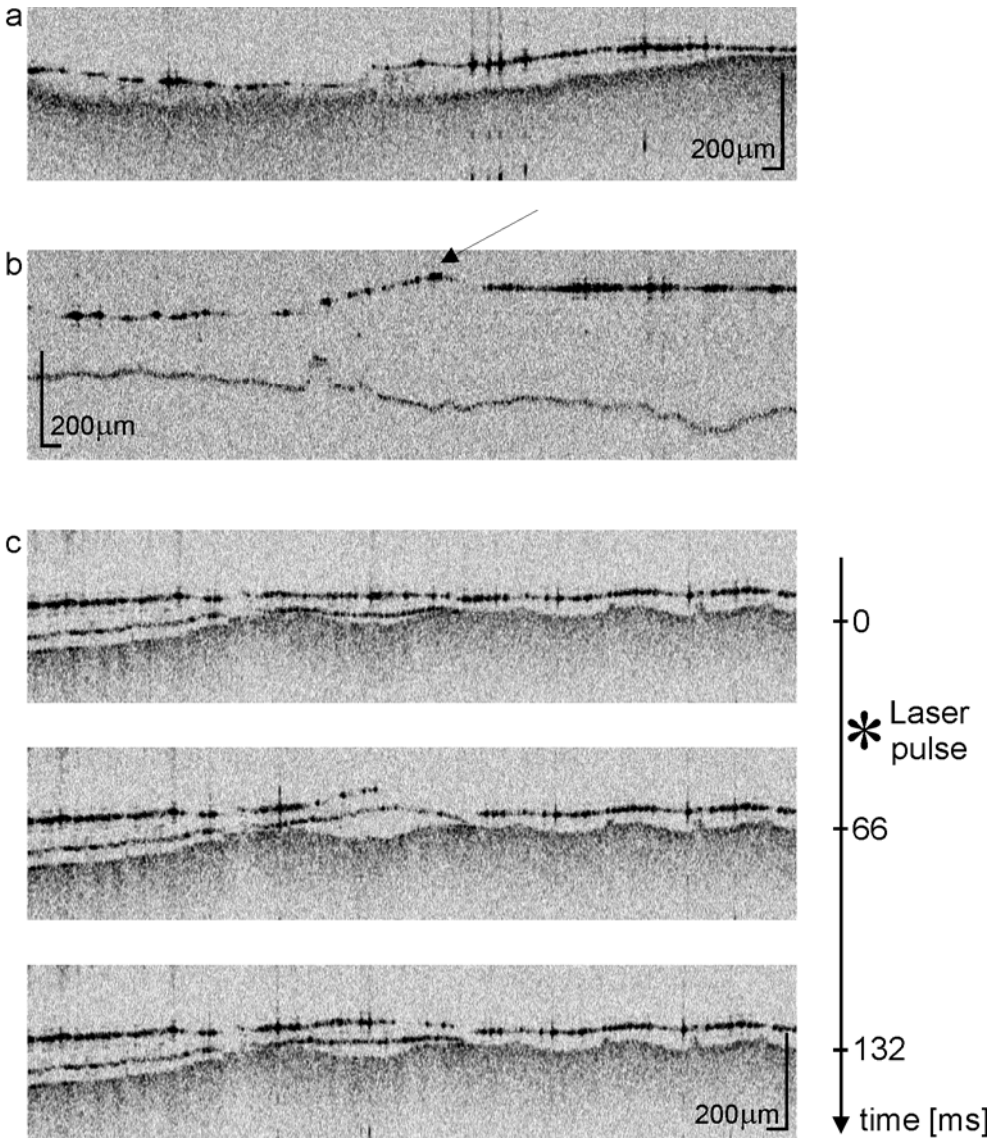

Fig. 6. OCT cross-sections of (a) the layer of Talens Picture Varnish Glossy 002 varnish during Er:YAG laser ablation with 1.2 J/cm2 fluence, and (b) the layer of Maimeri Dammar Matt Varnish with 2.3 J/cm^2 fluence. (c) Successive frames extracted from the OCT movie recorded during ablation of Talens Acrylic Varnish Mat with 1.2 J/cm^2 fluence. In all cases, the laser was working in short free-running mode, with a pulse frequency of 2 Hz. The recording rate was 15 frames/sec.

The fresh layer of Maimeri Dammar Matt Varnish behaves in a different way: a melting process rather than evaporation is predominant in this case, and occurs both below and above the ablation threshold. As can be seen in Figure 6b, some material has evaporated, but the presence of an elevated wave of liquid material (arrow), which precedes the ablation area, indicates the melting process. It should be noted that the elevation of the paint layer under the evaporated/melted varnish, visible in Fig. 6b, is merely an optical phenomenon caused by the change in optical distance to this surface. It indicates the decrease in the thickness of the varnish layer.

A third kind of reaction to the laser pulse is illustrated in Figure 6c. In this case, the Acrylic varnish seems to be more transparent to the IR laser radiation, so that the pulse energy is absorbed mostly at the paint surface, and exfoliation of the whole of the varnish layer takes place. In the figure, three successive frames selected from the OCT movie recorded during its ablation are shown. The laser pulse was applied between frames 1 and 2. Due to the strong dissipation of heat at the interface between paint and varnish, the whole varnish layer is significantly elevated. The next frame, taken 66

ms later, shows this layer somehow relaxed but still detached. Since the furthest left part of the cross-section was irradiated 4 seconds earlier, it is evident that the varnish layer remains permanently exfoliated.

Whole tomographic movies which from frames shown in figure 6 have been extracted are available an Electronic Supplementary Material (files: Ablation.avi, Exfoliation.avi, Melting.avi respectively).

4. Conclusions

The search for methods for non-invasive imaging of the structure of fragile objects of art is at present a strong focus of interest. Among other methods, Optical Coherence Tomography is still seeking its sustainable niche. In the case of statigraphy of paintings, although limited by the transparency of pigments to the light utilised, OCT may be considered as a method supplementary to previous techniques, but especially useful in examination of larger areas of the object than is possible or desirable with those. When compared with microphotography of a cross-section of a sample extirpated from the painting, it helps extend the knowledge of structure of the object to regions where sampling is not permitted or not practicable. It is especially important in the region of the author's signature. It has been shown that OCT enables resolution of the vertical position of the signature when it had been forged by painting on between two layers of varnish. It was also shown that, by recovering the profile of the paint layer covered by varnish, it is possible precisely to image a signature incised in fresh paint.

In the case of its use in the examination of stained glass, presented here for the first time, OCT can be useful due to its ability to image the structure of the glass non-destructively. Potentially, it could be utilised to evaluate deterioration of stained glass *in-situ*, without having to remove this historic glass out of its frame.

Another important application of Fourier domain OCT, related to its very high speed of imaging, is in monitoring dynamic processes. At present, it is possible to record a high density (and high resolution, if desired) OCT movie at a rate of 15 images per second. This is sufficiently fast to track the laser ablation of varnish, for example. Examples provided in this study show three behaviours of the layer ablated: true ablation, exfoliation, and melting with partial evaporation. However, whilst the present level of OCT technology does not permit real-time imaging of this quality, it is expected that, due the rapid growth of computer speed, this will soon be attainable.

In conclusion, it may be asserted with some conviction that, five years after the first reports on the utilisation of OCT for art diagnostic appeared, the list of present and possible OCT applications is quite long, but that there is still a plenty of room for new ideas and fields of utilisation.

Acknowledgements

The authors wish to thank Mr Antoni Rycyk for his assistance with the lasers, Mr Jerzy Graipel for providing samples of historic glass, and Ms Joanna Arszyńska for kind provision of the painting used in the signature investigations. The authors wish to thank Dr Robert Dale for critical reading the manuscript.

This work was supported by a Polish Government Research Grant through the years 2007 – 2009.

List of references

1. K. Groen, In: *The First Ten Years: The Examination and Conservation of Paintings, 1977 to 1987*, ed. by I. McClure (The Hamilton Kerr Institute of the Fitzwilliam Museum. University of Cambridge, Cambridge,1988) Vol. 1, pp. 48-65
2. W. C. McCrone, Journal of the American Institute for Conservation **33**, 101 (1994)

3. M.H. Butler, The microscope **21**, 101 (1973)

4. M.H. Butler, *Polarized Light Microscopy in the Conservation of Painting* (State Microscopical Society of Illinois, Chicago, 1970)

5. J.S. Martin, In *Postprints of the Wooden Artifacts Group* (Amer. Inst. for Conservation of Historic and Artistic Works, Wooden Artifacts Group 1996) pp. 19-21 –http://www.wag-eaic.org/1996/WAG_96_martin.pdf (Access date 13.03.2008)

6. N. Bäschlin, Zeitschrift für Kunsttechnologie und Konservierung **8**, 318 (1994)

7. K. Janssens and R. Van Grieken, *Non-destructive microanalysis of cultural heritage materials* (Elsevier, Amsterdam 2004)

8. E. Ciliberto and G. Spoto, *Modern Analytical Methods in Art and Archaeology* (John Wiley &Sons Canada Toronto 2000)

9. C. Lehanier, Mikrochimica Acta **104**, 245 (1991)

10. N. Khandekar, Reviews in Conservation **4**, 52 (2003)

11. M. Griesser, A. Denker, H. Musner, and K.H. Maier, in *Tradition and innovation: advances in conservation, Proceedings of the IIC Melbourne Congress, 10-14. Oct. 2000, Melbourne* (IIC London 2000) 82-87

12. S. Jane, R. Barker, and J. Chad, USA microscopy and analysis **55**, 31 (1995)

13. R. Barker, J. Chad, and S. Jane, The Picture Restorer **11**, 8 (1997)

14. A. R. Woll, D. H. Bilderback, S. Gruner, N. Gao, R. Huang, C. Bisulca, and J. Mass, in *Materials Issues in Art and Archaeology VII: Materials Research Society Symposium, November 30-December 3, 2004, Boston, Mass.* (Materials Research Society 2005) **852**, 281-290

15. P. Targowski, M. Góra, and M. Wojtkowski, Laser Chemistry **2006**, DOI:10.1155/2006/35373 http://www.hindawi.com/GetArticle.aspx?doi=10.1155/2006/35373 (2006)

16. P. Targowski, B. Rouba, M. Wojtkowski, I. Gorczyńska, and A. Kowalczyk, in *Ars longa – vita brevis, Tradycyjne i nowoczesne metody badania dzieł sztuki; Sesja naukowa poświęcona pamięci prof. Z. Borchwicza*, J. Flik Ed. (Wydawnictwo UMK Toruń 2003) 121 - 129

17. P. Targowski, B. Rouba, M. Wojtkowski, and A. Kowalczyk, Studies in Conservation **49**, 107 (2004)

18. M. L. Yang, C. W. Lu, I. J. Hsu, and C. C. Yang, Archeometry **46**, 171 (2004)

19. H. Liang, R. Cucu, G. M. Dobre, D. A. Jackson, J. Pedro, C. Pannell, D. Saunders, and A. G. Podoleanu, Proceedings SPIE **5502**, 378 (2004)

20. T. Arecchi, M. Bellini, and C. Corsi, Optics and Spectroscopy **101**, 23 (2006)

21. T. Arecchi, M. Bellini, C. Corsi, R. Fontana, M. Materazzi, L. Pezzati, and A. Tortora, Proceedings of SPIE **5857**, 278 (2005)

22. H. Liang, M. Cid, R. Cucu, G. Dobre, A. Podoleanu, J. Pedro, and D. Saunders, Optics Express **13**, 6133 (2005)

23. H. Liang, M. G. Cid, R. Cucu, G. Dobre, B. Kudimov, J. Pedro, D. Saunders, J. Cupitt, and A. Podoleanu, Proceedings SPIE **5857**, 261 (2005)

24. A. Szkulmowska, M. Góra, M. Targowska, B. Rouba, D. Stifter, E. Breuer, and P. Targowski, in *Lasers in the Conservation of Artworks, LACONA VI Proceedings, Vienna, Austria, Sept. 21 - 25, 2005*, J. Nimmrichter, W. Kautek, and M. Schreiner Ed. (Springer Verlag Berlin-Heidelberg-New York 2008) Series: Springer Proceedings in Physics, **116**, 487-492

25. B. Peric, S. Martin-Simpson, M. Spring, and H. Liang, in *Proceedings of Conservation Science 2007, Milan, 10-11th May 2007* (in press)

26. I. Gorczyńska, M. Wojtkowski, M. Szkulmowski, T. Bajraszewski, B. Rouba, A. Kowalczyk, and P. Targowski, in *Lasers in the Conservation of Artworks, LACONA VI Proceedings, Vienna, Austria, Sept. 21 - 25, 2005*, J. Nimmrichter, W. Kautek, and M. Schreiner Ed. (Springer Verlag Berlin-Heidelberg-New York 2008) Series: Springer Proceedings in Physics, **116**, 493-498

27. P. Targowski, T. Bajraszewski, I. Gorczyńska, M. Góra, A. Szkulmowska, M. Szkulmowski, M. Wojtkowski, J.J. Kałużny, B.J. Kałużny, and A. Kowalczyk, Optica Applicata **36**, 609 (2006)

28. T. Bajraszewski, I. Gorczyńska, B. Rouba, and P. Targowski, in *Lasers in the Conservation of Artworks, LACONA VI Proceedings, Vienna, Austria, Sept. 21 - 25, 2005*, J. Nimmrichter, W. Kautek, and M. Schreiner Ed. (Springer Verlag Berlin-Heidelberg-New York 2008) Series: Springer Proceedings in Physics, **116**, 507-512

29. P. Targowski, M. Góra, T. Bajraszewski, M. Szkulmowski, B. Rouba, T. Łękawa-Wysłouch, and L. Tymińska, Laser Chemistry **2006**, DOI:10.1155/2006/93658 http://www.hindawi.com/GetArticle.aspx?doi=10.1155/2006/93658 (2006)

30. M. Góra, P. Targowski, A. Rycyk, and J. Marczak, Laser Chemistry **2006**, DOI:10.1155/2006/10647http://www.hindawi.com/GetArticle.aspx?doi=10.1155/2006/10647 (2006)

31. M. Góra, A. Rycyk, J. Marczak, P. Targowski, and A. Kowalczyk, Proceedings SPIE **6429**, 64292V-1 (2007)

32. J. W. Goodman, *Statistical Optics* (Wiley New York 2000)

33. R. Leitgeb, C.K. Hitzenberger, and A.F. Fercher, Optics Express **11** (2003)

34. A. de Cruz, M. L. Wolbarsht, and S. A. Hauger, Journal of Cultural Heritage **1**, 173 (2000)

35. A. Andreotti, P. Bracco, M.P. Colombini, A. De Cruz, G. Lanterna, K. Nakahara, and F. Penaglia, in *Lasers in the Conservation of Artworks, LACONA VI Proceedings, Vienna, Austria, Sept. 21 - 25, 2005*, J. Nimmrichter, W. Kautek, and M. Schreiner Ed. (Springer Verlag Berlin-Heidelberg-New York 2008) Series: Springer Proceedings in Physics, **116**, 239-248

36. R. Bordalo, P.J. Morais, H. Gouveia, and Young C., Laser Chemistry **2006**, DOI:10.1155/2006/90279 http://www.hindawi.com/journals/lc/ (2006)

37. D. Anglos, S. Couris, and C. Fotakis, Applied Spectroscopy **51**, 1025 (1997)

38. Final Report CRAFT project ENV4-CT98-0787, http://www.art-innovation.nl/ventura/engine.php?Cmd=getpicture&P_site=316&P_self=213 (Access date: 25/06/2007)

39. P. Targowski, J. Marczak, M. Góra, A. Rycyk, and A. Kowalczyk, Proceedings SPIE **6618**, 661803-1 (2007)